Proceedings of the
Annual Stability Conference
Structural Stability Research Council
Nashville, Tennessee, March 24-27, 2015

Dynamic effects of geometric nonlinearity on inelastic frame behavior for seismic applications

Kevin K.F. Wong[1], Matthew S. Speicher[2]

Abstract
The traditional method of structural analysis with geometric nonlinearity uses small displacement theory with the linearized method of geometric stiffness or the approximate method of *P*-Δ stiffness to capture the reduction in stiffness due to axial forces in the columns of the structure. This often raises a stability question on whether these approaches can accurately predict large displacement response, such as nearing structural collapse in a major seismic event. In this research, the force analogy method combined with the stability functions formulated for nonlinear dynamic analysis will be used to answer this question. Through this combination, the stiffness force is computed by simply multiplying a nonlinear stiffness matrix (due to geometric nonlinearity using stability functions) with a nonlinear displacement vector (due to material nonlinearity using the force analogy method). Although this formulation is still based on small displacement theory, geometric nonlinearity is captured exactly using stability functions and therefore has a better chance of capturing the large displacement response more accurately than other small displacement approaches. A detailed derivation of the nonlinear dynamic analysis procedure using the state space method considering both geometric and material nonlinearity effects is presented to demonstrate the simplicity of the combined method in capturing the structural responses during seismic events.

1. Introduction

Buildings constructed in regions of high seismicity are vulnerable to strong ground shaking and thus are designed to sustain damage in a ductile fashion while maintaining load-carrying capacity. Nonlinear dynamic analysis is the most accurate method of capturing the response to seismic events, but this type of analysis requires creating computer models with nonlinear features that include both geometric and material nonlinearities. Furthermore, engineers often rely on numerical methods and software subroutines to handle the coupling effect of geometric and material nonlinearities, but software developers typically use their knowledge and preferences to make independent assumptions on what is best for their algorithms. For example, some software packages based on small displacement theory use a *P*-Δ stiffness matrix while others use a geometric stiffness matrix to address the effects of geometric nonlinearity. These

[1] Research Structural Engineer, National Institute of Standards and Technology, <kfwong@nist.gov>
[2] Research Structural Engineer, National Institute of Standards and Technology, <matthew.speicher@nist.gov>

differences can lead to inconsistencies in the predicted nonlinear response among software packages. This motivates the need for a critical review of the appropriate assumptions in treating material nonlinearities, geometric nonlinearities, and the coupling thereof.

In this research, an efficient analytical solution based on a theoretically consistent and rigorous derivation of the stiffness matrices for performing nonlinear dynamic analysis of structures is presented through the combined use of (1) the force analogy method, (2) stability functions, and (3) the state space method. The force analogy method is an efficient way of addressing material nonlinearity of framed structures with nonlinear hinge elements, where the global stiffness force after yielding is represented by a change in displacement instead of a change in stiffness (Wong and Hart, 1999a and 1999b; Wong and Wang, 2007a and 2007b; Wong 2011). In addition, stability functions provide the solution to geometric nonlinearity by capturing both large P-Δ and small P-δ effects by solving the fourth-order differential equation (Timoshenko and Gere, 1961; Horne and Merchant, 1965; Bazant and Cedolin, 2003; Park and Kim, 2008), which is intended to provide a higher level of accuracy than those that use the linearized versions of the small displacement theory. Finally, the state space method is an accurate numerical simulation tool for solving nonlinear dynamic problems (Aplevich, 1999; Friedland, 2005; Williams and Lawrence, 2007). Through the linkage of the force analogy method with stability functions, the stiffness force is computed by simply multiplying a nonlinear stiffness matrix with a nonlinear displacement vector for solving nonlinear *static* problems, which was presented in Wong (2014). In the present paper, this linkage is extended to solve *dynamic* problems by including the state space method into the procedure. To demonstrate the feasibility of the combined method, analysis results are compared with those obtained using various software packages based on small displacement theory or large displacement formulation that are available.

2. Force Analogy Method for Material Nonlinearity

In a structural dynamic analysis, the axial forces in columns are often varying with time (i.e., $P(t)$), and therefore the stiffness matrices due to geometric nonlinearity will also be functions of time. In order to explicitly include this effect in an analysis where the structure can also deform inelastically, the force analogy method (FAM) can be used. The concept of the FAM was derived in detail in Wong and Yang (1999), Hart and Wong (2000), and Li and Wong (2014) and was extended to include geometric nonlinearity using stability functions for nonlinear static analysis (Wong 2014). The details of the method are briefly summarized here with the incorporation of dynamic effects in the equations.

For a moment-resisting frame with *n* degrees of freedom (DOFs) and *m* plastic hinge locations (PHLs), the displacement relationship can be expressed as

$$\mathbf{x}(t) = \mathbf{x}'(t) + \mathbf{x}''(t) \tag{1}$$

where $\mathbf{x}(t)$ is the total displacement vector, $\mathbf{x}'(t)$ is the elastic displacement vector, and $\mathbf{x}''(t)$ is the inelastic displacement vector. Similar to the total displacements in Eq. 1, the total moment $\mathbf{m}(t)$ at the PHLs of a typical moment-resisting frame can be separated into elastic moment and inelastic moment, i.e.,

$$\mathbf{m}(t) = \mathbf{m}'(t) + \mathbf{m}''(t) \tag{2}$$

where $\mathbf{m}'(t)$ is the elastic moment due to the elastic displacement $\mathbf{x}'(t)$, and $\mathbf{m}''(t)$ is the inelastic moment due to the inelastic displacement $\mathbf{x}''(t)$. The displacements in Eq. 1 and moments in Eq. 2 are related by the following equations:

$$\mathbf{m}'(t) = \mathbf{K}'(t)^T \mathbf{x}'(t) \tag{3}$$

$$\mathbf{m}''(t) = -\left[\mathbf{K}''(t) - \mathbf{K}'(t)^T \mathbf{K}(t)^{-1} \mathbf{K}'(t)\right]\mathbf{\Theta}''(t) \tag{4}$$

where $\mathbf{\Theta}''$ is the plastic rotation at the PHLs, $\mathbf{K}(t)$ is the $n \times n$ global stiffness matrix, $\mathbf{K}'(t)$ is the $n \times m$ assembled stiffness matrix relating plastic rotations at the PHLs and forces at the DOFs, and $\mathbf{K}''(t)$ is the $m \times m$ assembled stiffness matrix relating plastic rotations with corresponding moments at the PHLs. For the *i*th beam or column member of the structure with plastic hinges at both ends but subjected to no axial force (or when geometric nonlinearity is ignored), the element stiffness matrices relating the shear and moment with lateral deformations can be written as:

$$\mathbf{K}_i(t) = \frac{EI}{L^3}\left[\begin{array}{cc|cc} 12 & 6L & -12 & 6L \\ 6L & 4L^2 & -6L & 2L^2 \\ \hline -12 & -6L & 12 & -6L \\ 6L & 2L^2 & -6L & 4L^2 \end{array}\right] \quad , \quad \mathbf{K}'_i(t) = \frac{EI}{L^2}\left[\begin{array}{cc} 6 & 6 \\ 4L & 2L \\ \hline -6 & -6 \\ 2L & 4L \end{array}\right] \quad , \quad \mathbf{K}''_i(t) = \frac{EI}{L}\begin{bmatrix} 4 & 2 \\ 2 & 4 \end{bmatrix} \tag{5}$$

where E is the elastic modulus, I is the moment of inertia, and L is the length of the *i*th beam or column member. When geometric nonlinearity is considered, stability functions can be used. After solving for a fourth-order differential equation with appropriate boundary conditions (Wong 2014), the *i*th member stiffness matrices similar to those shown in Eq. 5 become:

$$\mathbf{K}_i(t) = \frac{EI}{L^3}\left[\begin{array}{cc|cc} s' & \bar{s}L & -s' & \bar{s}L \\ \bar{s}L & sL^2 & -\bar{s}L & scL^2 \\ \hline -s' & -\bar{s}L & s' & -\bar{s}L \\ \bar{s}L & scL^2 & -\bar{s}L & sL^2 \end{array}\right] \quad , \quad \mathbf{K}'_i(t) = \frac{EI}{L^2}\left[\begin{array}{cc} \bar{s} & \bar{s} \\ sL & scL \\ \hline -\bar{s} & -\bar{s} \\ scL & sL \end{array}\right] \quad , \quad \mathbf{K}''_i(t) = \frac{EI}{L}\begin{bmatrix} s & sc \\ sc & s \end{bmatrix} \tag{6}$$

where

$$s = \frac{\lambda(\sin\lambda - \lambda\cos\lambda)}{2 - 2\cos\lambda - \lambda\sin\lambda} \quad , \quad c = \frac{\lambda - \sin\lambda}{\sin\lambda - \lambda\cos\lambda} \tag{7a}$$

$$\bar{s} = s + sc = \frac{\lambda^2(1-\cos\lambda)}{2 - 2\cos\lambda - \lambda\sin\lambda} \quad , \quad s' = 2\bar{s} - \lambda^2 = \frac{\lambda^3\sin\lambda}{2 - 2\cos\lambda - \lambda\sin\lambda} \tag{7b}$$

and $\lambda = \sqrt{P_i(t)/EI} \times L$, with $P_i(t)$ denoting the axial compressive force of the *i*th beam or column member. Substituting Eqs. 3 and 4 into Eq. 2 and rearranging the terms, the first governing equation of the FAM for dynamic analysis is obtained as follows:

$$\mathbf{m}(t) + \mathbf{K}''(t)\mathbf{\Theta}''(t) = \mathbf{K}'(t)^T \mathbf{x}(t) \tag{8}$$

The second governing equation of the FAM relates the inelastic displacement $\mathbf{x}''(t)$ at the DOFs and the plastic rotation $\mathbf{\Theta}''(t)$ in the PHLs. This equation can be written as

$$\mathbf{x}''(t) = \mathbf{K}(t)^{-1}\mathbf{K}'(t)\mathbf{\Theta}''(t) \tag{9}$$

3. Geometric Nonlinearity Considerations in Structural Analysis

When the FAM is used, the stiffness force in the equation of motion is calculated by multiplying the stiffness matrix $\mathbf{K}(t)$ with the elastic displacement $\mathbf{x}'(t)$. For an n-DOF system subjected to earthquake ground motions, this equation can be written as

$$\mathbf{M}\ddot{\mathbf{x}}(t) + \mathbf{C}\dot{\mathbf{x}}(t) + \mathbf{K}(t)\mathbf{x}'(t) = -\mathbf{M}\mathbf{g}(t) - \mathbf{F}_a(t) \tag{10}$$

where $\mathbf{M}$ is the $n \times n$ invertible mass matrix, $\mathbf{C}$ is the $n \times n$ damping matrix, $\dot{\mathbf{x}}(t)$ is the $n \times 1$ velocity vector, $\ddot{\mathbf{x}}(t)$ is the $n \times 1$ acceleration vector, $\mathbf{g}(t)$ is the $n \times 1$ earthquake ground acceleration vector corresponding to the effect of ground motion at each DOF, and $\mathbf{F}_a(t)$ is the $n \times 1$ vector of additional forces imposed on the frame due to geometric nonlinearity of the gravity columns (mainly the P-Δ effect). This effect can often be modeled using a leaning column (or sometimes called a P-Δ column) in a two-dimensional analysis but requires detailed modeling of all gravity columns in a three-dimensional analysis. In a two-dimensional analysis, the relationship between this lateral force $\mathbf{F}_a(t)$ and the lateral displacement can be written as:

$$\mathbf{F}_a(t) = \mathbf{K}_a\mathbf{x}(t) \tag{11}$$

where $\mathbf{K}_a$ is an $n \times n$ stiffness matrix that is a function of the gravity loads on the leaning column and the corresponding story height, but it is not a function of time. For two-dimensional frames with horizontal degrees of freedom only, this $\mathbf{K}_a$ matrix often takes the form:

$$\mathbf{K}_a = \begin{bmatrix} -Q_1/h_1 - Q_2/h_2 & Q_2/h_2 & 0 & \cdots & 0 \\ Q_2/h_2 & -Q_2/h_2 - Q_3/h_3 & \ddots & \ddots & \vdots \\ 0 & \ddots & \ddots & Q_{n-1}/h_{n-1} & 0 \\ \vdots & \ddots & Q_{n-1}/h_{n-1} & -Q_{n-1}/h_{n-1} - Q_n/h_n & Q_n/h_n \\ 0 & \cdots & 0 & Q_n/h_n & -Q_n/h_n \end{bmatrix} \tag{12}$$

where Q_i is the axial force due to gravity on the leaning column of the *i*th floor, and h_i is the story height of the *i*th floor.

While the lateral force $\mathbf{F}_a(t)$ takes care of the nonlinear geometric effects from all the gravity columns, the stiffness matrix $\mathbf{K}(t)$ in Eq. 10 must consider both large P-Δ and small P-δ effects on the moment-resisting frame itself. Let this time-dependent global stiffness matrix $\mathbf{K}(t)$ be represented in the form:

$$\mathbf{K}(t) = \mathbf{K}_L + \mathbf{K}_G(t) \tag{13}$$

where $\mathbf{K}_L$ denotes the linearized elastic stiffness of the frame due to the gravity loads only, and $\mathbf{K}_G(t)$ denotes the change in stiffness due to the change in axial load on members during the dynamic loading. Note that the $\mathbf{K}_L$ matrix is a constant stiffness matrix computed by using only the gravity loads on the columns of the moment-resisting frame (which means $\mathbf{K}_L = \mathbf{K}(t_0) = \mathbf{K}(0)$, i.e., the stiffness matrix computed at time step 0) and therefore it is not a function of time. Thus, only having to compute the linearized elastic stiffness matrix once is one of the advantages of using the FAM in the nonlinear response history analysis.

A case study is here presented to illustrate the currently available approaches that can be used to consider geometric nonlinearity. Let the single degree of freedom (SDOF) column as shown in Fig. 1a be subjected to a constant axial compressive force *P*. Let the mass be *M*, damping be *C*, elastic modulus be *E*, moment of inertia be *I*, and length be *L*. The degree of freedom is set up so that the mass is restrained from rotation, but it is free to translate in the horizontal direction.

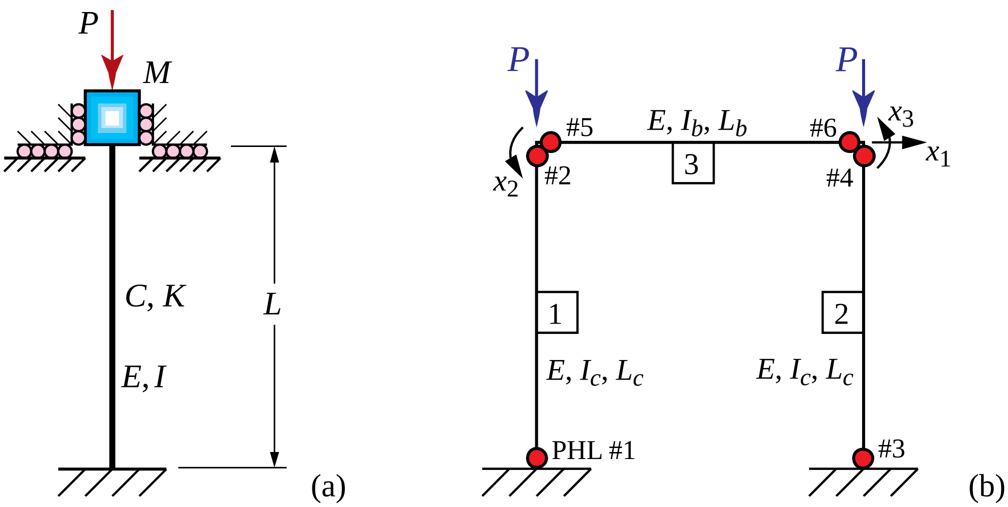

Figure 1: Single degree of freedom models with geometric nonlinearity

Based on this set up, the column experiences a constant axial force due to the gravity load only and also experiences shear and moment due to the earthquake ground motion only. Therefore, the lateral stiffness of the column will remain constant with a constant axial force during the entire earthquake time history analysis. If geometric nonlinearity is totally ignored in this problem, the lateral stiffness related to the horizontal translation degree of freedom at the top of the column is simply:

$$K_{OR} = \frac{12EI}{L^3} \tag{14}$$

where K_{OR} represents the original stiffness of the SDOF system without considering any geometric nonlinearities. If geometric nonlinearity is considered using the *P*-Δ approach, the lateral stiffness of the SDOF column becomes:

$$K_{P\Delta} = \frac{12EI}{L^3} - \frac{P}{L} \tag{15}$$

where $K_{P\Delta}$ denotes the geometrically nonlinear stiffness of the column using the *P*-Δ approach (i.e., including large *P*-Δ effect but excluding small *P*-δ effect). If geometric nonlinearity is considered using the geometric stiffness approach, the lateral stiffness of the SDOF column becomes:

$$K_{GS} = \frac{12EI}{L^3} - \frac{6P}{5L} \tag{16}$$

where K_{GS} denotes the geometrically nonlinear stiffness of the column using the geometric stiffness approach (i.e., including both large P-Δ and small P-δ effects). Finally, if geometric nonlinearity is considered through the use of stability functions, the stiffness matrix becomes:

$$K_{SF} = \frac{s'EI}{L^3} \tag{17}$$

where K_{SF} denotes the geometrically nonlinear stiffness computed using the stability functions approach (i.e., including both large P-Δ and small P-δ effects in a consistent form), and s' is the stability coefficients defined in Eq. 7b.

In this study, let $E = 100$ GPa, $I = 20 \times 10^6$ mm^4, $L = 4$ m, and $P = 500$ kN in compression. Using a mass of $M = 9{,}500$ kg, the calculated stiffnesses and the corresponding periods of vibration are summarized in Table 1. Note that the critical buckling load for the SDOF column is $P_{cr} = \pi^2 EI / L^2 = 1{,}234$ kN, and therefore the applied load is at 40.5% of the critical buckling load (i.e., $P / P_{cr} = 0.405$). At this axial compressive force level, it is observed that $K_{GS} \approx K_{SF}$, but there is a 11.5% difference in stiffness between $K_{P\Delta}$ and K_{SF}. This means ignoring the small P-δ effect results in an increase in lateral stiffness of 11.5%. Table 1 also shows that the difference between using $K_{P\Delta}$ and using K_{SF} results in a 5.3% difference in the calculated period of vibration of the SDOF column.

Table 1: Comparison of geometric nonlinear stiffnesses, periods, and maximum responses

	Stiffness (kN/m)	Period (s)	Max Displacement (m)	Max Velocity (m/s)	Max Acceleration (*g*)
K_{OR}	375.0	1.000	0.4226	2.617	1.704
$K_{P\Delta}$	250.0	1.225	0.4074	2.208	1.095
K_{GS}	225.0	1.291	0.5035	2.606	1.218
K_{SF}	224.3	1.293	0.5056	2.610	1.218

Assuming 2% damping, the SDOF column shown in Fig. 1a is subjected to the 1995 Kobe earthquake as shown in Fig. 2. The resulting displacement responses using the original stiffness, P-Δ stiffness, geometric stiffness, and stability function stiffness are presented in Fig. 3 by using the state space method (SSM) to be presented in Section 4. In addition, the absolute maximum displacement, velocity, and absolute acceleration for using various geometric nonlinear stiffness approaches are summarized in Table 1. It can be seen from Fig. 3 that the responses using K_{GS} match those using K_{SF} well even at such a large axial compressive force, and Table 1 shows that the difference in maximum displacement response is only 0.4%. However, there are more noticeable differences between the responses using $K_{P\Delta}$ and those using K_{SF}, where the maximum displacement response using $K_{P\Delta}$ reduces by 19% and the maximum acceleration response also reduces by 10%.

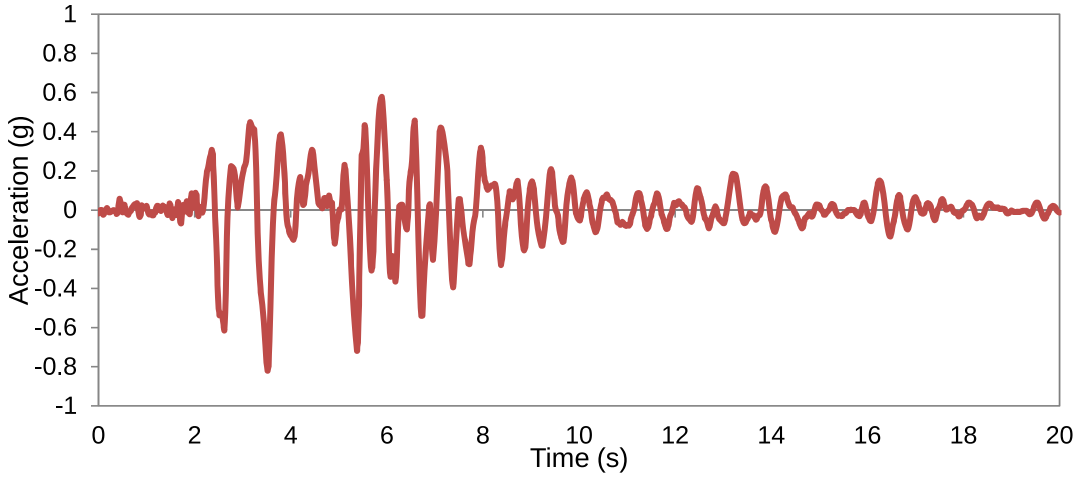

Figure 2: 1995 Kobe earthquake ground acceleration time history

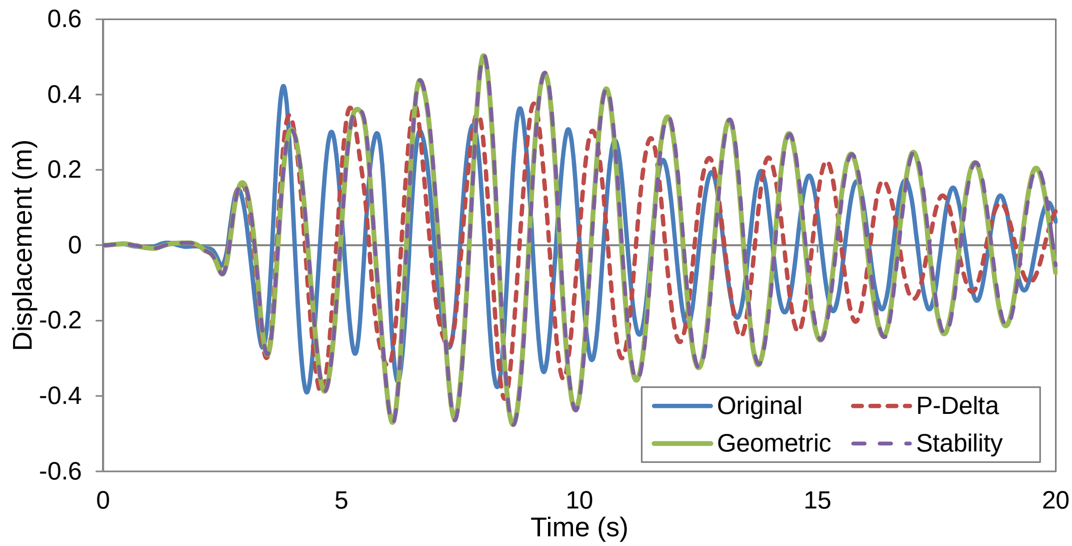

Figure 3: Displacement responses of the SDOF column using different stiffnesses

Knowing the stiffness of the column is important because it can be used to assess the type of geometric nonlinearity that is embedded in various software packages. Consider the same SDOF column as shown in Fig. 1a with 0% damping is modeled using four small-displacement software packages (randomly labeled as S1, S2, S3, and S4) and is subjected to the 1995 Kobe earthquake shown in Fig. 2. Fig. 4 shows the exact match between the current analysis method using SSM with K_{GS} and the software packages S1 and S4. Similarly, Fig. 5 shows the exact match between the current analysis method using SSM with $K_{P\Delta}$ and software packages S2 and S3. This indicates half of the small-displacement software packages use geometric stiffness that considers both large P-Δ and small P-δ effects in the formulation, while the other half of the small-displacement software packages use P-Δ stiffness that considers only large P-Δ effects and ignores the small P-δ effects. Note that even though using 0% damping is an idealized situation, it helps eliminate the potentially differing effects of using damping parameters on the responses that may occur due to differences in damping formulations used in various software packages.

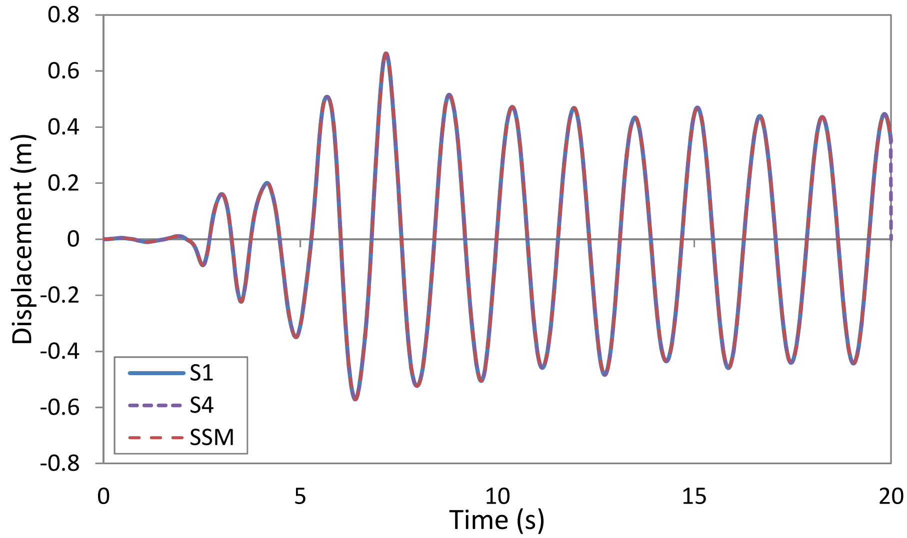

Figure 4: Displacement response comparison for the state space method (SSM) using K_{GS} with other software packages that use geometric stiffness approach

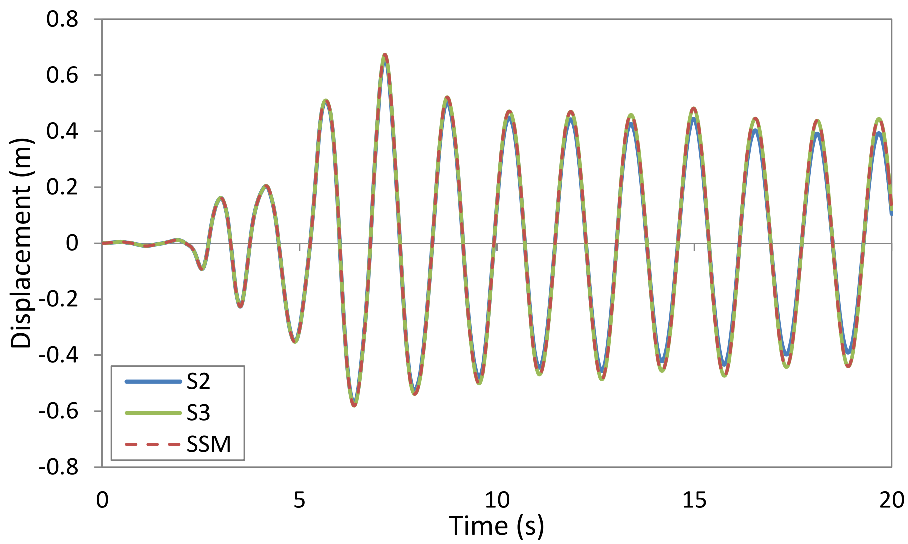

Figure 5: Displacement response comparison for the state space method (SSM) using $K_{P\Delta}$ with other software packages that use P-Δ stiffness approach

4. State Space Method

The state space method (SSM) is an accurate and efficient analysis tool for solving dynamic problems, and the explicit formulation is used in this research. It requires that the mass matrix be invertible. However, in many practical structural analysis problems, masses at certain DOFs are intentionally set to zero in order to reduce the number of DOFs in the structural model. When the mass is zero at certain DOFs, such as those DOFs related to the vertical translation and joint rotations, the mass matrix in Eq. 10 will become singular and not be invertible. This causes a problem in the state space formulation for dynamic analysis because it requires an invertible mass matrix for solving the differential equation. To overcome this problem with non-invertible mass matrix, static condensation is first applied in order to eliminate those DOFs with zero mass or mass moment of inertia before representing the equation of motion in the state space form.

4.1 Static Condensation for State Space Dynamic Analysis

Consider a moment-resisting frame with *n* DOFs and *m* PHLs as presented in Eq. 10, the equation of motion can be partitioned in the matrix form as

$$\begin{bmatrix} \mathbf{M}_{dd} & \mathbf{0} \\ \mathbf{0} & \mathbf{0} \end{bmatrix} \begin{Bmatrix} \ddot{\mathbf{x}}_d(t) \\ \ddot{\mathbf{x}}_r(t) \end{Bmatrix} + \begin{bmatrix} \mathbf{C}_{dd} & \mathbf{0} \\ \mathbf{0} & \mathbf{0} \end{bmatrix} \begin{Bmatrix} \dot{\mathbf{x}}_d(t) \\ \dot{\mathbf{x}}_r(t) \end{Bmatrix} + \begin{bmatrix} \mathbf{K}_{dd}(t) & \mathbf{K}_{dr}(t) \\ \mathbf{K}_{rd}(t) & \mathbf{K}_{rr}(t) \end{bmatrix} \begin{Bmatrix} \mathbf{x}'_d(t) \\ \mathbf{x}'_r(t) \end{Bmatrix} = -\begin{bmatrix} \mathbf{M}_{dd} & \mathbf{0} \\ \mathbf{0} & \mathbf{0} \end{bmatrix} \begin{Bmatrix} \mathbf{g}_d(t) \\ \mathbf{0} \end{Bmatrix} - \begin{Bmatrix} \mathbf{F}_a(t) \\ \mathbf{0} \end{Bmatrix} \tag{18}$$

where $\mathbf{M}_{dd}$ is the mass matrix associated with translational DOFs with mass only, $\mathbf{C}_{dd}$ is the damping matrix associated with translational DOFs with mass only, and $\mathbf{K}_{dd}(t)$, $\mathbf{K}_{dr}(t)$, $\mathbf{K}_{rd}(t)$, and $\mathbf{K}_{rr}(t)$ are the stiffness sub-matrices partitioned according to the DOFs with mass and those with zero mass. Note that the stiffness sub-matrices are functions of time, since these matrices depend on the axial compressive force in the columns which are also functions of time. The vector $\mathbf{x}'(t)$ is the elastic displacement response, $\dot{\mathbf{x}}(t)$ is the velocity response, $\ddot{\mathbf{x}}(t)$ is the acceleration response, $\mathbf{F}_a(t)$ is the $d \times 1$ vector of additional forces imposed on the translational DOFs due to geometric nonlinearity of gravity columns, and the earthquake ground acceleration vector $\mathbf{g}_d(t)$ corresponds to the effect of a ground motion at each DOF associated with nonzero mass. The subscript *d* denotes the number of degrees of freedom that have nonzero mass, and subscript *r* denotes the number of degrees of freedom that have zero mass and zero moment of inertia. This gives $n = d + r$ in an *n*-DOF system.

The governing equations of the FAM presented in Eqs. 8 and 9 can similarly be partitioned as follows:

$$\mathbf{m}(t) + \mathbf{K}''(t)\boldsymbol{\Theta}''(t) = \begin{bmatrix} \mathbf{K}'_d(t)^T & \mathbf{K}'_r(t)^T \end{bmatrix} \begin{Bmatrix} \mathbf{x}_d(t) \\ \mathbf{x}_r(t) \end{Bmatrix} \tag{19}$$

$$\begin{Bmatrix} \mathbf{x}''_d(t) \\ \mathbf{x}''_r(t) \end{Bmatrix} = \begin{bmatrix} \mathbf{K}_{dd}(t) & \mathbf{K}_{dr}(t) \\ \mathbf{K}_{rd}(t) & \mathbf{K}_{rr}(t) \end{bmatrix}^{-1} \begin{bmatrix} \mathbf{K}'_d(t) \\ \mathbf{K}'_r(t) \end{bmatrix} \boldsymbol{\Theta}''(t) \tag{20}$$

where

$$\mathbf{K}'(t) = \begin{bmatrix} \mathbf{K}'_d(t) \\ \mathbf{K}'_r(t) \end{bmatrix} \quad , \quad \mathbf{x}''(t) = \begin{Bmatrix} \mathbf{x}''_d(t) \\ \mathbf{x}''_r(t) \end{Bmatrix} \quad , \quad \begin{Bmatrix} \mathbf{x}_d(t) \\ \mathbf{x}_r(t) \end{Bmatrix} = \begin{Bmatrix} \mathbf{x}'_d(t) \\ \mathbf{x}'_r(t) \end{Bmatrix} + \begin{Bmatrix} \mathbf{x}''_d(t) \\ \mathbf{x}''_r(t) \end{Bmatrix} \tag{21}$$

Static condensation is now performed. First consider Eq. 18. By performing static condensation, the second equation of Eq. 18 is extracted and written in the long form as

$$\mathbf{K}_{rd}(t)\mathbf{x}'_d(t) + \mathbf{K}_{rr}(t)\mathbf{x}'_r(t) = \mathbf{0} \tag{22}$$

Solving for $\mathbf{x}_r'(t)$ in Eq. 22 gives

$$\mathbf{x}_r'(t) = -\mathbf{K}_{rr}^{-1}(t)\mathbf{K}_{rd}(t)\mathbf{x}_d'(t) \tag{23}$$

Now substituting Eq. 23 back into the first equation of Eq. 18 gives

$$\mathbf{M}_{dd}\ddot{\mathbf{x}}_d(t) + \mathbf{C}_{dd}\dot{\mathbf{x}}_d(t) + \mathbf{K}_{dd}(t)\mathbf{x}_d'(t) - \mathbf{K}_{dr}(t)\mathbf{K}_{rr}^{-1}(t)\mathbf{K}_{rd}(t)\mathbf{x}_d'(t) = -\mathbf{M}_{dd}\mathbf{g}_d(t) - \mathbf{F}_a(t) \tag{24}$$

Define

$$\overline{\mathbf{K}}(t) = \mathbf{K}_{dd}(t) - \mathbf{K}_{dr}(t)\mathbf{K}_{rr}^{-1}(t)\mathbf{K}_{rd}(t) \tag{25}$$

Then Eq. 24 becomes

$$\mathbf{M}_{dd}\ddot{\mathbf{x}}_d(t) + \mathbf{C}_{dd}\dot{\mathbf{x}}_d(t) + \overline{\mathbf{K}}(t)\mathbf{x}_d'(t) = -\mathbf{M}_{dd}\mathbf{g}_d(t) - \mathbf{F}_a(t) \tag{26}$$

which represents the equation of motion in the statically condensed form. Similarities can be observed between Eq. 10 and Eq. 26. The $\mathbf{M}$, $\mathbf{C}$, and $\mathbf{K}(t)$ matrices in Eq. 10 have been replaced by $\mathbf{M}_{dd}$, $\mathbf{C}_{dd}$, and $\overline{\mathbf{K}}(t)$ matrices in Eq. 26, respectively, and the $\mathbf{x}'(t)$, $\dot{\mathbf{x}}(t)$, and $\ddot{\mathbf{x}}(t)$ vectors in Eq. 10 have been replaced by $\mathbf{x}_d'(t)$, $\dot{\mathbf{x}}_d(t)$, and $\ddot{\mathbf{x}}_d(t)$ vectors in Eq. 26, respectively. Therefore, Eq. 26 shows that only those DOFs with mass need to be considered in the state space method of dynamic analysis.

However, Eqs. 19 and 20 contain both DOFs with mass (i.e., $\mathbf{x}_d(t)$ and $\mathbf{x}_d''(t)$) and DOFs without mass (i.e., $\mathbf{x}_r(t)$ and $\mathbf{x}_r''(t)$). Therefore, static condensation must also be applied to these two equations to reduce the DOFs to those with mass only. First consider Eq. 20. Pre-multiplying both sides of Eq. 20 by the stiffness matrix $\mathbf{K}(t)$ gives

$$\left[\begin{array}{c|c} \mathbf{K}_{dd}(t) & \mathbf{K}_{dr}(t) \\ \hline \mathbf{K}_{rd}(t) & \mathbf{K}_{rr}(t) \end{array}\right]\left\{\begin{array}{c} \mathbf{x}_d''(t) \\ \hline \mathbf{x}_r''(t) \end{array}\right\} = \left[\begin{array}{c} \mathbf{K}_d' \\ \hline \mathbf{K}_r' \end{array}\right]\mathbf{\Theta}''(t) \tag{27}$$

Extracting the second equation of Eq. 27 and solving for $\mathbf{x}_r''(t)$ gives

$$\mathbf{x}_r''(t) = -\mathbf{K}_{rr}^{-1}(t)\mathbf{K}_{rd}(t)\mathbf{x}_d''(t) + \mathbf{K}_{rr}^{-1}(t)\mathbf{K}_r'(t)\mathbf{\Theta}''(t) \tag{28}$$

Now substituting Eq. 28 back into the first equation of Eq. 27 gives

$$\mathbf{K}_{dd}(t)\mathbf{x}_d''(t) + \mathbf{K}_{dr}(t)\left[-\mathbf{K}_{rr}^{-1}(t)\mathbf{K}_{rd}(t)\mathbf{x}_d''(t) + \mathbf{K}_{rr}^{-1}(t)\mathbf{K}_r'(t)\mathbf{\Theta}''(t)\right] = \mathbf{K}_d'\mathbf{\Theta}''(t) \tag{29}$$

and rearranging the terms gives

$$\left[\mathbf{K}_{dd}(t) - \mathbf{K}_{dr}(t)\mathbf{K}_{rr}^{-1}(t)\mathbf{K}_{rd}(t)\right]\mathbf{x}_d''(t) = \left[\mathbf{K}_d'(t) - \mathbf{K}_{dr}(t)\mathbf{K}_{rr}^{-1}(t)\mathbf{K}_r'(t)\right]\mathbf{\Theta}''(t) \tag{30}$$

Define

$$\overline{\mathbf{K}}'(t) = \mathbf{K}_d'(t) - \mathbf{K}_{dr}(t)\mathbf{K}_{rr}^{-1}(t)\mathbf{K}_r'(t) \tag{31}$$

Substituting Eqs. 25 and 31 into Eq. 30 gives

$$\overline{\mathbf{K}}(t)\mathbf{x}''_d(t) = \overline{\mathbf{K}}'(t)\mathbf{\Theta}''(t) \tag{32}$$

Finally, pre-multiplying both sides of Eq. 32 by the inverse of the condensed stiffness matrix (i.e., $\overline{\mathbf{K}}(t)^{-1}$) gives

$$\mathbf{x}''_d(t) = \overline{\mathbf{K}}(t)^{-1}\overline{\mathbf{K}}'(t)\mathbf{\Theta}''(t) \tag{33}$$

which represents the second governing equations of the FAM in the statically condensed form. Similarities can also be observed between Eq. 9 and Eq. 33. The $\mathbf{K}(t)$ and $\mathbf{K}'(t)$ matrices in Eq. 9 have been replaced by $\overline{\mathbf{K}}(t)$ and $\overline{\mathbf{K}}'(t)$ matrices in Eq. 33, respectively, and the $\mathbf{x}''(t)$ vector in Eq. 9 have been replaced by $\mathbf{x}''_d(t)$ vector in Eq. 33.

Finally, consider Eq. 19. Expanding the right hand side of Eq. 19 gives

$$\mathbf{m}(t) + \mathbf{K}''(t)\mathbf{\Theta}''(t) = \mathbf{K}'_d(t)^T\mathbf{x}_d(t) + \mathbf{K}'_r(t)^T\mathbf{x}_r(t) \tag{34}$$

In Eq. 34, the term $\mathbf{x}_r(t)$ must be first calculated. Since $\mathbf{x}_r(t) = \mathbf{x}'_r(t) + \mathbf{x}''_r(t)$ according to Eq. 21, substituting Eqs. 23 and 28 into this equation gives

$$\mathbf{x}_r(t) = \mathbf{x}'_r(t) + \mathbf{x}''_r(t) = -\mathbf{K}_{rr}^{-1}(t)\mathbf{K}_{rd}(t)\mathbf{x}'_d(t) - \mathbf{K}_{rr}^{-1}(t)\mathbf{K}_{rd}(t)\mathbf{x}''_d(t) + \mathbf{K}_{rr}^{-1}(t)\mathbf{K}'_r(t)\mathbf{\Theta}''(t) \tag{35}$$

Also, since $\mathbf{x}'_d(t) + \mathbf{x}''_d(t) = \mathbf{x}_d(t)$ according to Eq. 21, substituting this result in Eq. 35 gives

$$\mathbf{x}_r(t) = -\mathbf{K}_{rr}^{-1}(t)\mathbf{K}_{rd}(t)\mathbf{x}_d(t) + \mathbf{K}_{rr}^{-1}(t)\mathbf{K}'_r(t)\mathbf{\Theta}''(t) \tag{36}$$

Now substituting Eq. 36 into Eq. 34 and rearranging the terms gives

$$\mathbf{m}(t) + \left[\mathbf{K}''(t) - \mathbf{K}'_r(t)^T\mathbf{K}_{rr}^{-1}(t)\mathbf{K}'_r(t)\right]\mathbf{\Theta}''(t) = \left[\mathbf{K}'_d(t)^T - \mathbf{K}'_r(t)^T\mathbf{K}_{rr}^{-1}(t)\mathbf{K}_{rd}(t)\right]\mathbf{x}_d(t) \tag{37}$$

Define

$$\overline{\mathbf{K}}''(t) = \mathbf{K}''(t) - \mathbf{K}'_r(t)^T\mathbf{K}_{rr}^{-1}(t)\mathbf{K}'_r(t) \tag{38}$$

Substituting Eqs. 31 and 38 into Eq. 37 gives

$$\mathbf{m}(t) + \overline{\mathbf{K}}''(t)\mathbf{\Theta}''(t) = \overline{\mathbf{K}}'(t)^T\mathbf{x}_d(t) \tag{39}$$

which represents the first governing equation of the FAM in the statically condensed form. Similarities can again be observed between Eq. 8 and Eq. 39. The $\mathbf{K}'(t)$ and $\mathbf{K}''(t)$ matrices in Eq. 8 have been replaced by $\overline{\mathbf{K}}'(t)$ and $\overline{\mathbf{K}}''(t)$ matrices in Eq. 39, respectively, and the $\mathbf{x}(t)$ vector in Eq. 8 have been replaced by $\mathbf{x}_d(t)$ vector in Eq. 39.

In summary, Eq. 26 represents the equation of motion and Eqs. 39 and 33 represent the first and second governing equations of the FAM, respectively, in the statically condensed form.

4.2 State Space Method for Nonlinear Dynamic Analysis

By applying static condensation to eliminate the DOFs associated with zero mass and zero mass moment of inertia, the resulting equations for nonlinear dynamic analysis with the FAM are presented in Eqs. 26, 39, and 33, which are rewritten here:

$$\mathbf{M}_{dd}\ddot{\mathbf{x}}_d(t)+\mathbf{C}_{dd}\dot{\mathbf{x}}_d(t)+\overline{\mathbf{K}}(t)\mathbf{x}'_d(t)=-\mathbf{M}_{dd}\mathbf{g}_d(t)-\mathbf{F}_a(t) \tag{40a}$$

$$\mathbf{m}(t)+\overline{\mathbf{K}}''(t)\mathbf{\Theta}''(t)=\overline{\mathbf{K}}'(t)^T\mathbf{x}_d(t) \tag{40b}$$

$$\mathbf{x}''_d(t)=\overline{\mathbf{K}}(t)^{-1}\overline{\mathbf{K}}'(t)\mathbf{\Theta}''(t) \tag{40c}$$

where

$$\overline{\mathbf{K}}(t)=\mathbf{K}_{dd}(t)-\mathbf{K}_{dr}(t)\mathbf{K}_{rr}^{-1}(t)\mathbf{K}_{rd}(t) \tag{41a}$$

$$\overline{\mathbf{K}}'(t)=\mathbf{K}'_d(t)-\mathbf{K}_{dr}(t)\mathbf{K}_{rr}^{-1}(t)\mathbf{K}'_r(t) \tag{41b}$$

$$\overline{\mathbf{K}}''(t)=\mathbf{K}''(t)-\mathbf{K}'_r(t)^T\mathbf{K}_{rr}^{-1}(t)\mathbf{K}'_r(t) \tag{41c}$$

and Eqs. 11 and 13 can be written in the forms:

$$\mathbf{F}_a(t)=\mathbf{K}_a\mathbf{x}_d(t) \quad , \quad \overline{\mathbf{K}}(t)=\overline{\mathbf{K}}_L+\overline{\mathbf{K}}_G(t) \tag{42}$$

First solving for the elastic displacement $\mathbf{x}'_d(t)$ in Eq. 21 and substituting the result into Eq. 40a gives

$$\mathbf{M}_{dd}\ddot{\mathbf{x}}_d(t)+\mathbf{C}_{dd}\dot{\mathbf{x}}_d(t)+\overline{\mathbf{K}}(t)\mathbf{x}_d(t)=-\mathbf{M}_{dd}\mathbf{g}_d(t)-\mathbf{F}_a(t)+\overline{\mathbf{K}}(t)\mathbf{x}''_d(t) \tag{43}$$

Then substituting Eq. 42 into Eq. 43, the equation of motion after considering both large *P*-Δ and small *P*-δ effects of geometric nonlinearity of the entire structure becomes

$$\mathbf{M}_{dd}\ddot{\mathbf{x}}_d(t)+\mathbf{C}_{dd}\dot{\mathbf{x}}_d(t)+\overline{\mathbf{K}}_L\mathbf{x}_d(t)=-\mathbf{M}_{dd}\mathbf{g}_d(t)-\mathbf{K}_a\mathbf{x}_d(t)-\overline{\mathbf{K}}_G(t)\mathbf{x}_d(t)+\overline{\mathbf{K}}(t)\mathbf{x}''_d(t) \tag{44}$$

Define

$$\overline{\mathbf{K}}_e=\overline{\mathbf{K}}_L+\mathbf{K}_a \tag{45}$$

where $\overline{\mathbf{K}}_e$ represents the elastic stiffness of the entire structure, which is the sum of the linearized elastic stiffness $\overline{\mathbf{K}}_L$ of the frame only and the additional stiffness $\mathbf{K}_a$ induced by the gravity columns. Substituting Eq. 45 into Eq. 44, it follows that

$$\mathbf{M}_{dd}\ddot{\mathbf{x}}_d(t)+\mathbf{C}_{dd}\dot{\mathbf{x}}_d(t)+\overline{\mathbf{K}}_e\mathbf{x}_d(t)=-\mathbf{M}_{dd}\mathbf{g}_d(t)-\overline{\mathbf{K}}_G(t)\mathbf{x}_d(t)+\overline{\mathbf{K}}(t)\mathbf{x}''_d(t) \tag{46}$$

Let the material nonlinearity term (i.e., $\overline{\mathbf{K}}(t)\mathbf{x}''_d(t)$) and geometric nonlinearity term (i.e., $-\overline{\mathbf{K}}_G(t)\mathbf{x}_d(t)$) shown on the right hand side of Eq. 46 be treated as the equivalent forces applied to the structure, the equation can now be solved using the state space method.

To represent Eq. 46 in state space form, let the state vector $\mathbf{z}(t)$ be defined as

$$\mathbf{z}(t) = \begin{Bmatrix} \mathbf{x}_d(t) \\ \dot{\mathbf{x}}_d(t) \end{Bmatrix} \tag{47}$$

which is a $2n \times 1$ vector with a collection of states of the responses. It follows from Eq. 46 that

$$\begin{aligned} \dot{\mathbf{z}}(t) = \begin{Bmatrix} \dot{\mathbf{x}}_d(t) \\ \ddot{\mathbf{x}}_d(t) \end{Bmatrix} &= \begin{bmatrix} \mathbf{0} & \mathbf{I} \\ -\mathbf{M}_{dd}^{-1}\overline{\mathbf{K}}_e & -\mathbf{M}_{dd}^{-1}\mathbf{C}_{dd} \end{bmatrix} \begin{Bmatrix} \mathbf{x}_d(t) \\ \dot{\mathbf{x}}_d(t) \end{Bmatrix} \\ &+ \begin{bmatrix} \mathbf{0} \\ -\mathbf{h} \end{bmatrix} \mathbf{a}(t) + \begin{bmatrix} \mathbf{0} \\ \mathbf{M}_{dd}^{-1} \end{bmatrix} \left(\overline{\mathbf{K}}_e(t)\mathbf{x}''_d(t) - \overline{\mathbf{K}}_G(t)\mathbf{x}_d(t) \right) \end{aligned} \tag{48}$$

where $\mathbf{h}$ is an $n \times 3$ matrix that relates the directions of each DOF with the global *X*-, *Y*-, and *Z*-directions (i.e., a collection of 0's and 1's in all entries), and $\mathbf{a}(t)$ is the 3×1 ground acceleration vector in the three global directions of $g_X(t)$, $g_Y(t)$, and $g_Z(t)$. The relationship between the ground acceleration vector $\mathbf{g}_d(t)$ for each DOF in Eq. 46 and the three-component ground acceleration vector $\mathbf{a}(t)$ in Eq. 47 can be expressed as

$$\mathbf{g}_d(t) = \mathbf{h}\mathbf{a}(t) = \mathbf{h} \begin{Bmatrix} g_X(t) \\ g_Y(t) \\ g_Z(t) \end{Bmatrix} \tag{49}$$

To simplify Eq. 48, let

$$\mathbf{A} = \begin{bmatrix} \mathbf{0} & \mathbf{I} \\ -\mathbf{M}_{dd}^{-1}\overline{\mathbf{K}}_e & -\mathbf{M}_{dd}^{-1}\mathbf{C}_{dd} \end{bmatrix} \quad , \quad \mathbf{H} = \begin{bmatrix} \mathbf{0} \\ -\mathbf{h} \end{bmatrix} \quad , \quad \mathbf{B} = \begin{bmatrix} \mathbf{0} \\ -\mathbf{M}_{dd}^{-1} \end{bmatrix} \tag{50a}$$

$$\mathbf{f}_G(t) = -\overline{\mathbf{K}}_G(t)\mathbf{x}_d(t) \quad , \quad \mathbf{f}_M(t) = \overline{\mathbf{K}}(t)\mathbf{x}''_d(t) \tag{50b}$$

where $\mathbf{A}$ is the $2d \times 2d$ state transition matrix in the continuous form, $\mathbf{H}$ is the $2d \times 3$ ground motion transition matrix in the continuous form, $\mathbf{B}$ is the $2d \times d$ nonlinearity transition matrix in the continuous form, $\mathbf{f}_G(t)$ is the $d \times 1$ equivalent force vector due to geometric nonlinearity, and $\mathbf{f}_M(t)$ is the $d \times 1$ equivalent force vector due to material nonlinearity. Then Eq. 48 becomes

$$\dot{\mathbf{z}}(t) = \mathbf{A}\mathbf{z}(t) + \mathbf{H}\mathbf{a}(t) + \mathbf{B}\mathbf{f}_G(t) + \mathbf{B}\mathbf{f}_M(t) \tag{51}$$

Solving for the first-order linear differential equation in Eq. 51 gives

$$\mathbf{z}(t) = \mathbf{e}^{\mathbf{A}(t-t_o)}\mathbf{z}(t_o) + \mathbf{e}^{\mathbf{A}t}\int_{t_o}^{t} \mathbf{e}^{-\mathbf{A}s}\left[\mathbf{H}\mathbf{a}(s) + \mathbf{B}\mathbf{f}_G(s) + \mathbf{B}\mathbf{f}_M(s)\right]ds \tag{52}$$

where t_o is the time of reference when the integration begins, which is typically the time when the states are known. In a recursive analysis procedure, the known states are often taken at the current time step $\mathbf{z}(t_o)$ and the objective is to calculate the states at the next time step $\mathbf{z}(t)$.

To integrate Eq. 52 numerically, let $t_{k+1} = t$, $t_k = t_o$, and $\Delta t = t_{k+1} - t_k$, and the subscript k denotes the kth time step, then it follows from Eq. 52 that

$$\mathbf{z}_{k+1} = \mathbf{e}^{\mathbf{A}\Delta t}\mathbf{z}_k + \mathbf{e}^{\mathbf{A}t_{k+1}}\int_{t_k}^{t_{k+1}} \mathbf{e}^{-\mathbf{A}s}\left[\mathbf{Ha}(s) + \mathbf{Bf}_G(s) + \mathbf{Bf}_M(s)\right]ds \tag{53}$$

Using the delta function approximation for the variables in the integral, where the ground acceleration vector $\mathbf{a}(s)$, equivalent geometric nonlinear force vector $\mathbf{f}_G(s)$, and equivalent material nonlinear force vector $\mathbf{f}_M(s)$ take the form:

$$\mathbf{a}(s) = \mathbf{a}_k\delta(s - t_k)\Delta t \quad , \quad t_k \le s < t_{k+1} \tag{54a}$$

$$\mathbf{f}_G(s) = \mathbf{f}_{G,k}\delta(s - t_k)\Delta t \quad , \quad t_k \le s < t_{k+1} \tag{54b}$$

$$\mathbf{f}_M(s) = \mathbf{f}_{M,k}\delta(s - t_k)\Delta t \quad , \quad t_k \le s < t_{k+1} \tag{54c}$$

Substituting Eq. 54 into Eq. 53 and performing the integration gives

$$\mathbf{z}_{k+1} = \mathbf{e}^{\mathbf{A}\Delta t}\mathbf{z}_k + \Delta t\mathbf{e}^{\mathbf{A}\Delta t}\mathbf{Ha}_k + \Delta t\mathbf{e}^{\mathbf{A}\Delta t}\mathbf{Bf}_{G,k} + \Delta t\mathbf{e}^{\mathbf{A}\Delta t}\mathbf{Bf}_{M,k} \tag{55}$$

where $\mathbf{z}_k$, $\mathbf{a}_k$, $\mathbf{f}_{G,k}$, and $\mathbf{f}_{M,k}$ are the discretized forms of $\mathbf{z}(t)$, $\mathbf{a}(t)$, $\mathbf{f}_G(t)$, and $\mathbf{f}_M(t)$, respectively. Let

$$\mathbf{F}_d = \mathbf{e}^{\mathbf{A}\Delta t} \quad , \quad \mathbf{H}_d = \mathbf{e}^{\mathbf{A}\Delta t}\mathbf{H}\Delta t \quad , \quad \mathbf{B}_d = \mathbf{e}^{\mathbf{A}\Delta t}\mathbf{B}\Delta t \tag{56}$$

Then Eq. 55 becomes

$$\mathbf{z}_{k+1} = \mathbf{F}_d\mathbf{z}_k + \mathbf{H}_d\mathbf{a}_k + \mathbf{B}_d\mathbf{f}_{G,k} + \mathbf{B}_d\mathbf{f}_{M,k} \tag{57}$$

In Eq. 57, both equivalent force terms $\mathbf{f}_{G,k}$ and $\mathbf{f}_{M,k}$ are functions of the column axial forces at time step k. Therefore, Eq. 57 represents the recursive equation for calculating the dynamic response of moment-resisting framed structures while considering updates on geometric nonlinearity as the axial compressive force in columns changes with time.

For the case when updates on geometric nonlinearity are ignored in the nonlinear dynamic analysis, the $\overline{\mathbf{K}}_G(t)$ matrix as given in Eq. 42 becomes $\overline{\mathbf{K}}_G(t) = \mathbf{0}$. Therefore, from the same equation, $\overline{\mathbf{K}}(t) = \overline{\mathbf{K}}_o$. Then it follows from Eq. 50b that

$$\mathbf{f}_G(t) = \left[\mathbf{0}\right]\cdot\mathbf{x}_d(t) = \mathbf{0} \tag{58a}$$

$$\mathbf{f}_M(t) = \overline{\mathbf{K}}(t)\mathbf{x}''_d(t) = \overline{\mathbf{K}}_o\mathbf{x}''_d(t) \tag{58b}$$

and Eq. 57 becomes

$$\mathbf{z}_{k+1} = \mathbf{F}_d\mathbf{z}_k + \mathbf{H}_d\mathbf{a}_k + \mathbf{G}_d\mathbf{x}''_{d,k} \tag{59}$$

where

$$\mathbf{G}_d = \mathbf{B}_d \overline{\mathbf{K}}_o = \mathbf{e}^{\mathbf{A}\Delta t} \begin{bmatrix} \mathbf{0} \\ \mathbf{M}_{dd}^{-1} \end{bmatrix} \overline{\mathbf{K}}_o \Delta t = \mathbf{e}^{\mathbf{A}\Delta t} \begin{bmatrix} \mathbf{0} \\ \mathbf{M}_{dd}^{-1} \overline{\mathbf{K}}_o \end{bmatrix} \Delta t \tag{60}$$

with $\mathbf{x}''_{d,k}$ representing the discretized forms of $\mathbf{x}''_d(t)$. Eq. 59 represents the recursive equation for calculating the nonlinear dynamic response of moment-resisting framed structures without updates on geometric nonlinearity as the axial compressive force in columns changes with time.

To perform nonlinear dynamic analysis, either Eq. 57 or Eq. 59 is used in conjunction with the governing equations of the FAM (see Eqs. 40b and 40c), rewritten here in discretized forms:

$$\mathbf{m}_{k+1} + \overline{\mathbf{K}}''_{k+1} \Delta\mathbf{\Theta}'' = \overline{\mathbf{K}}'^{T}_{k+1} \mathbf{x}_{d,k+1} - \overline{\mathbf{K}}''_{k+1} \mathbf{\Theta}''_k \tag{61}$$

$$\mathbf{x}''_{d,k+1} = \overline{\mathbf{K}}_{k+1}^{-1} \overline{\mathbf{K}}'_{k+1} \mathbf{\Theta}''_{k+1} \tag{62}$$

where $\mathbf{x}_{d,k}$, $\mathbf{\Theta}''_k$, and $\mathbf{m}_k$ are the discretized forms of $\mathbf{x}_d(t)$, $\mathbf{\Theta}''(t)$, and $\mathbf{m}(t)$, respectively, $\Delta\mathbf{\Theta}'' = \mathbf{\Theta}''_{k+1} - \mathbf{\Theta}''_k$, and $\overline{\mathbf{K}}_k$, $\overline{\mathbf{K}}'_k$, and $\overline{\mathbf{K}}''_k$ are the stiffness matrices at time step k computed using the axial forces in columns at the same time step. Note that the stiffness matrices in Eqs. 61 and 62 are written in terms of time step $k+1$. However, the axial forces in columns at time step $k+1$ is unknown prior to the calculation of moments and change in plastic rotations, which means Eq. 61 requires an iterative procedure in the solution and may be difficult to execute. Therefore, the stiffness matrices in these two equations may often be replaced by those at time step k without loss of accuracy, i.e.,

$$\mathbf{m}_{k+1} + \overline{\mathbf{K}}''_k \Delta\mathbf{\Theta}'' = \overline{\mathbf{K}}'^{T}_k \mathbf{x}_{k+1} - \overline{\mathbf{K}}''_k \mathbf{\Theta}''_k \tag{63}$$

$$\mathbf{x}''_{k+1} = \overline{\mathbf{K}}_k^{-1} \overline{\mathbf{K}}'_k \mathbf{\Theta}''_{k+1} \tag{64}$$

If updates to geometric nonlinearity are ignored, these stiffness matrices become:

$$\overline{\mathbf{K}}_k = \overline{\mathbf{K}}(0) = \overline{\mathbf{K}}_o \quad , \quad \overline{\mathbf{K}}'_k = \overline{\mathbf{K}}'(0) = \overline{\mathbf{K}}'_o \quad , \quad \overline{\mathbf{K}}''_k = \overline{\mathbf{K}}''(0) = \overline{\mathbf{K}}''_o \tag{65}$$

Then Eqs. 63 and 64 become

$$\mathbf{m}_{k+1} + \overline{\mathbf{K}}''_o \Delta\mathbf{\Theta}'' = \overline{\mathbf{K}}'^{T}_o \mathbf{x}_{d,k+1} - \overline{\mathbf{K}}''_o \mathbf{\Theta}''_k \tag{66}$$

$$\mathbf{x}''_{d,k+1} = \overline{\mathbf{K}}_o^{-1} \overline{\mathbf{K}}'_o \mathbf{\Theta}''_{k+1} \tag{67}$$

Eqs. 59, 66, and 67 represent the set of equations for solving the nonlinear dynamic analysis problems when no update to geometric nonlinearity due to changes in axial force is performed.

Finally, the absolute acceleration vector (i.e., $\ddot{\mathbf{y}}_d(t) = \ddot{\mathbf{x}}_d(t) + \mathbf{g}_d(t)$) can be computed by rewriting Eq. 10 in discretized form as

$$\ddot{\mathbf{y}}_{d,k} = -\mathbf{M}_{dd}^{-1} \mathbf{C}_{dd} \dot{\mathbf{x}}_{d,k} - \mathbf{M}_{dd}^{-1} \overline{\mathbf{K}}_k \left(\mathbf{x}_{d,k} - \mathbf{x}''_{d,k} \right) - \mathbf{M}_{dd}^{-1} \mathbf{K}_a \mathbf{x}_{d,k} \tag{68}$$

where $\dot{\mathbf{x}}_{d,k}$ and $\ddot{\mathbf{y}}_{d,k}$ are the discretized forms of $\dot{\mathbf{x}}_d(t)$ and $\ddot{\mathbf{y}}_d(t)$, respectively.

5. Implementation of the Combined Method on a One-Story Frame

As an example of the above rigorous formulation, consider a one-story one-bay moment-resisting frame as shown in Fig. 1b with members assumed to be axially rigid. This gives a total of 3 DOFs (i.e., $n = 3$) and 6 PHLs (i.e., $m = 6$) as shown in the figure. Assuming no update of geometric nonlinearity due to changes in axial forces in columns is performed, then the global stiffness matrices $\mathbf{K}$, $\mathbf{K}'$, and $\mathbf{K}''$ become

$$\mathbf{K} = \left[\begin{array}{ccc} (s_1' + s_2')EI_c/L_c^3 & \bar{s}_1 EI_c/L_c^2 & \bar{s}_2 EI_c/L_c^2 \\ \bar{s}_1 EI_c/L_c^2 & s_1 EI_c/L_c + 4EI_b/L_b & 2EI_b/L_b \\ \bar{s}_2 EI_c/L_c^2 & 2EI_b/L_b & s_2 EI_c/L_c + 4EI_b/L_b \end{array}\right] \begin{array}{l} \leftarrow x_1 \\ \leftarrow x_2 \\ \leftarrow x_3 \end{array} \tag{69a}$$

$$\mathbf{K}' = \left[\begin{array}{cc|cc|cc} \bar{s}_1 EI_c/L_c^2 & \bar{s}_1 EI/L_c^2 & \bar{s}_2 EI_c/L_c^2 & \bar{s}_2 EI_c/L_c^2 & 0 & 0 \\ s_1 c_1 EI_c/L_c & s_1 EI_c/L_c & 0 & 0 & 4EI_b/L_b & 2EI_b/L_b \\ 0 & 0 & s_2 c_2 EI_c/L_c & s_2 EI_c/L_c & 2EI_b/L_b & 4EI_b/L_b \end{array}\right] \begin{array}{l} \leftarrow x_1 \\ \leftarrow x_2 \\ \leftarrow x_3 \end{array} \tag{69b}$$

$$\mathbf{K}'' = \left[\begin{array}{cc|cc|cc} s_1 EI_c/L_c & s_1 c_1 EI_c/L_c & 0 & 0 & 0 & 0 \\ s_1 c_1 EI_c/L_c & s_1 EI_c/L_c & 0 & 0 & 0 & 0 \\ \hline 0 & 0 & s_2 EI_c/L_c & s_2 c_2 EI_c/L_c & 0 & 0 \\ 0 & 0 & s_2 c_2 EI_c/L_c & s_2 EI_c/L_c & 0 & 0 \\ \hline 0 & 0 & 0 & 0 & 4EI_b/L_b & 2EI_b/L_b \\ 0 & 0 & 0 & 0 & 2EI_b/L_b & 4EI_b/L_b \end{array}\right] \begin{array}{l} \leftarrow \theta_1'' \\ \leftarrow \theta_2'' \\ \leftarrow \theta_3'' \\ \leftarrow \theta_4'' \\ \leftarrow \theta_5'' \\ \leftarrow \theta_6'' \end{array} \tag{69c}$$

where s_i, c_i, $\bar{s}_i$, and s_i' are stability coefficients of the ith column computed using Eq. 7.

Assume that the frame has a mass of $M_{dd} = 318.7$ Mg and a damping of 0% (i.e., $C_{dd} = 0.0$) at DOF #1, while the mass moment of inertia at DOFs #2 and #3 are ignored. This gives $d = 1$ and $r = 2$. Note that $d + r = n$. Therefore, static condensation can be applied to eliminate the DOFs for x_2 and x_3. Let $E = 200$ GPa, $I_b = I_c = 4.995\times10^8$ mm^4, $L_b = 7.62$ m, and $L_c = 4.57$ m. Using Eq. 41 with an assumed gravity load of $P = 5{,}338$ kN, the condensed stiffness matrices $\overline{\mathbf{K}}_o$, $\overline{\mathbf{K}}_o'$, and $\overline{\mathbf{K}}_o''$ become:

$$\overline{K}_o = \overline{K}_e = 10{,}018 \text{ kN/m} \tag{70a}$$

$$\overline{\mathbf{K}}_o' = \left[16{,}907 \quad 11{,}331 \quad 16{,}907 \quad 11{,}331 \quad -11{,}331 \quad -11{,}331\right] \text{ kN} \tag{70b}$$

$$\overline{\mathbf{K}}_o'' = \left[\begin{array}{cccccc} 56{,}761 & 13{,}494 & 2{,}458 & 4{,}585 & -13{,}494 & -4{,}585 \\ 13{,}494 & 25{,}173 & 4{,}585 & 8{,}554 & -25{,}173 & -8{,}554 \\ 2{,}458 & 4{,}585 & 56{,}761 & 13{,}494 & -4{,}585 & -13{,}494 \\ 4{,}585 & 8{,}554 & 13{,}494 & 25{,}173 & -8{,}554 & -25{,}173 \\ -13{,}494 & -25{,}173 & -4{,}585 & -8{,}554 & 25{,}173 & 8{,}554 \\ -4{,}585 & -8{,}554 & -13{,}494 & -25{,}173 & 8{,}554 & 25{,}173 \end{array}\right] \text{ kN-m/rad} \tag{70c}$$

The period of vibration T is calculated as:

$$T = 2\pi\sqrt{M_{dd}/\overline{K}_o} = 2\pi\sqrt{318.7/10{,}017} = 1.121 \text{ s} \tag{71}$$

With a time step size of $\Delta t = 0.01$ s and assuming no updates to the geometric nonlinearity is performed (i.e., Eqs. 59, 66, and 67 are used), the transition matrices are calculated as:

$$\mathbf{A} = \begin{bmatrix} 0 & 1 \\ -31.43 & 0 \end{bmatrix} \quad , \quad \mathbf{H} = \begin{bmatrix} 0 \\ -1 \end{bmatrix} \quad , \quad \mathbf{B} = \begin{bmatrix} 0 \\ 0.5495 \end{bmatrix} \tag{72a}$$

$$\mathbf{F}_d = \mathbf{e}^{\mathbf{A}\Delta t} = \begin{bmatrix} 0.998429 & 0.009995 \\ -0.31415 & 0.998429 \end{bmatrix} \ , \ \mathbf{H}_d = \begin{bmatrix} -0.00010 \\ -0.00998 \end{bmatrix} \ , \ \mathbf{G}_d = \begin{bmatrix} 0.00314 \\ 0.31381 \end{bmatrix} \tag{72b}$$

and Eqs. 59, 66, and 67 for performing the nonlinear dynamic analysis using the state space method become

$$\begin{Bmatrix} x_1 \\ \dot{x}_1 \end{Bmatrix}_{k+1} = \begin{bmatrix} 0.998429 & 0.009995 \\ -0.31415 & 0.998429 \end{bmatrix} \begin{Bmatrix} x_1 \\ \dot{x}_1 \end{Bmatrix}_k + \begin{bmatrix} -0.00010 \\ -0.00998 \end{bmatrix} a_k + \begin{bmatrix} 0.00314 \\ 0.31381 \end{bmatrix} x''_{d,k} \tag{73a}$$

$$\begin{Bmatrix} m_1 \\ m_2 \\ m_3 \\ m_4 \\ m_5 \\ m_6 \end{Bmatrix}_{k+1} + \overline{\mathbf{K}}''_o \begin{Bmatrix} \Delta\theta''_1 \\ \Delta\theta''_2 \\ \Delta\theta''_3 \\ \Delta\theta''_4 \\ \Delta\theta''_5 \\ \Delta\theta''_6 \end{Bmatrix} = \begin{bmatrix} 16{,}907 \\ 11{,}331 \\ 16{,}907 \\ 11{,}331 \\ -11{,}331 \\ -11{,}331 \end{bmatrix} x_{1,k+1} - \overline{\mathbf{K}}''_o \begin{Bmatrix} \theta''_1 \\ \theta''_2 \\ \theta''_3 \\ \theta''_4 \\ \theta''_5 \\ \theta''_6 \end{Bmatrix}_k \tag{73b}$$

$$x''_{d,k+1} = \frac{1}{10{,}017} \begin{bmatrix} 16{,}907 & 11{,}331 & 16{,}907 & 11{,}331 & -11{,}331 & -11{,}331 \end{bmatrix} \begin{Bmatrix} \theta''_1 \\ \theta''_2 \\ \theta''_3 \\ \theta''_4 \\ \theta''_5 \\ \theta''_6 \end{Bmatrix}_{k+1} \tag{73c}$$

where $\overline{\mathbf{K}}''_o$ in Eq. 73b is given in Eq. 70c. Eq. 73 represents the set of recursive equations that is used for the entire nonlinear dynamic analysis. Note that the method for solving Eq. 73b has been discussed extensively in Wong (2014) and therefore it is not repeated here.

Assume that the plastic hinges exhibit elastic-plastic behavior with plastic moment capacities of $m_b = 3{,}130$ kN-m for the beam and $m_c = 3{,}909$ kN-m for the two columns. By subjecting the frame to the 1995 Kobe earthquake ground motion as shown in Fig. 2 with a scale factor of 1.3, the global displacement response at DOF #1 is plotted in Fig. 6. In addition, the same undamped responses obtained from a software package that uses geometric stiffness (GS) and from another software package that uses P-Δ stiffness (PDS) are plotted in the figure for comparison. It is observed that the state space method (SSM) produces reasonable response in comparison with other software packages that use different geometric nonlinearity formulations. Besides geometric nonlinearity, the difference in responses may also be attributed to the lack of consistency in the P-M-θ'' interaction after hinging of columns among the software packages and the currently proposed state space method of analysis.

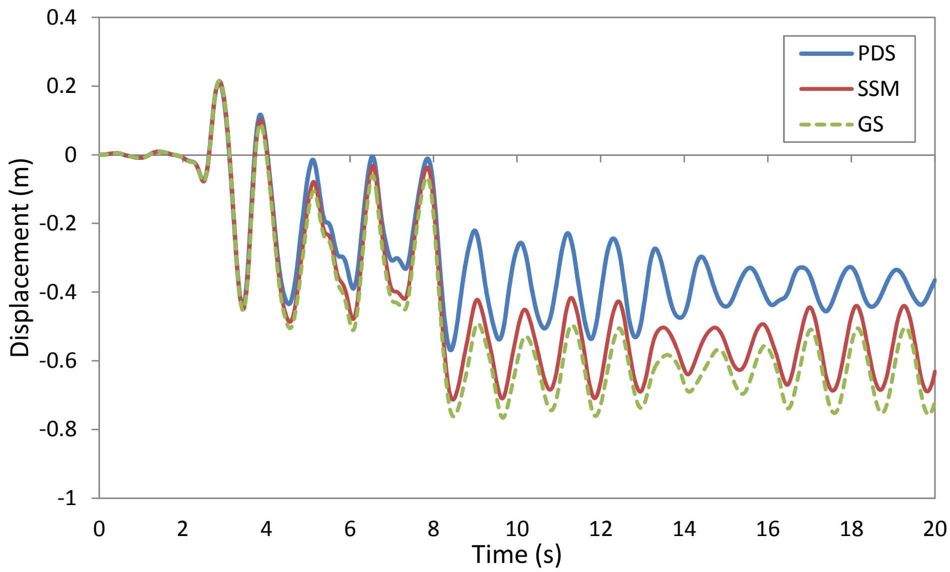

Figure 6: Displacement response of a one-story frame using the state space method (SSM) as compared to other software packages

6. Four-Story Moment-Resisting Frame

Consider the four-story moment-resisting steel frame as shown in Fig. 7. This frame originally contains 36 DOFs (i.e., $n = 36$). Assume that no mass or mass moment of inertia is assigned to all vertical translation DOFs and all rotation DOFs. After applying static condensation, the structural model is left with 4 DOFs (i.e., $d = 4$) and 56 PHLs (i.e., $m = 56$). Assume a mass of 72,670 kg is used on each floor, and a gravity load of 863 kN is applied on each exterior column member and 1,263 k is applied on each interior column member. In addition, 0% damping is assumed to provide a better comparison of the response with other software packages, including a software package that uses P-Δ stiffness (PDS) and a software package that uses large displacement formulation (LDF).

Assume the yield stress of the member is 345 MPa and all 56 plastic hinges exhibit elastic-plastic behavior. The steel frame is now subjected to the 1995 Kobe earthquake ground motion as shown in Fig. 2 with scaling factors of 0.6, 0.8, 1.0, and 1.2. The roof displacement responses are summarized in Fig. 8. Based on the results, it is observed that the responses computed using state space method (SSM) with stability functions match very closely with those obtained from using large displacement formulation (LDF), each at a roof displacement of about 0.8 m over a height of 18.6 m (or a drift ratio of 4.3%). This suggests that the proposed nonlinear analysis method of rigorously capturing both large P-Δ and small P-δ effects can approximate large displacement response quite accurately.

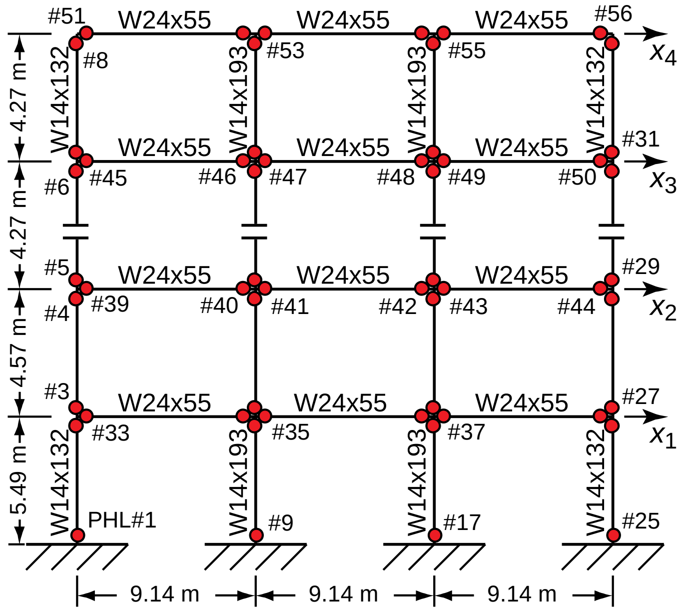

Figure 7: Four-story moment-resisting steel frame

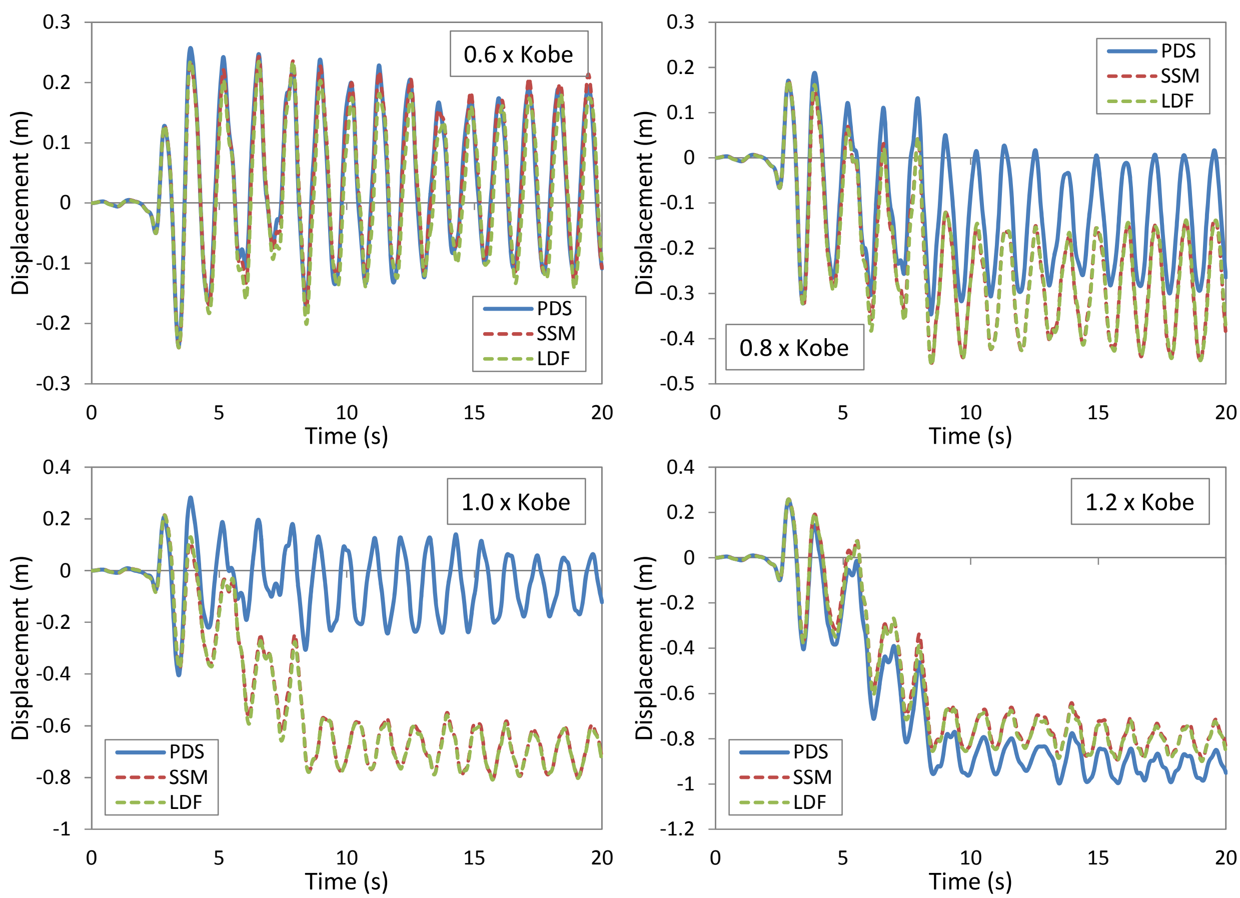

Figure 8: Roof displacement response of the four-story frame using the state space method (SSM) as compared to other software packages

7. Conclusion

In this paper, a detailed derivation using stability functions to aid in performing nonlinear dynamic analysis of framed structures was presented with an addition to the state space method of analysis. Through this derivation, it was demonstrated that the stiffness force can be computed by simply multiplying a geometric nonlinear stiffness matrix with a material nonlinear displacement vector, which in turn is used in the dynamic equilibrium equation of motion. Based on studies using SDOF systems, the use of stability functions produced the global stiffness matrix that was numerically equivalent to the commonly used geometric stiffness approach while having the advantage of capturing the small P-δ effect exactly. This helps the currently proposed method of using small-displacement theory to more closely align with more rigorous analysis software that uses large-displacement formulations. In other words, if more accurate analysis is needed but the cost of using large-displacement formulations is not justified, the solution method herein provides a way to improve the analysis. However, further research is necessary in order to determine the limitation of small-displacement theory and when large-displacement formulations are needed.

References

Aplevich, J.D. (1999). *The Essentials of Linear State-Space Systems*, John Wiley & Sons, New York.

Bazant, Z.P., Cedolin, L. (2003). *Stability of Structures*, Dover Publication, New York.

Friedland, B. (2005) *Control System Design: An Introduction to State-Space Methods*, Dover Publications, New York.

Hart, G.C., Wong, K. (2000). *Structural Dynamics for Structural Engineers*, John Wiley & Sons, New York.

Horne, M.Z., Merchant, W. (1965). *The Stability of Frames*, Pergamon Press, New York.

Li, G., Wong, K.K.F. (2014). *Theory of Nonlinear Structural Analysis: The Force Analogy Method for Earthquake Engineering*, John Wiley & Sons, Singapore.

Park, J.W., Kim, S.E. (2008). "Nonlinear inelastic analysis of steel-concrete composite beam-columns using the stability functions." *Structural Engineering and Mechanics*, 30 (6) 763-785.

Timoshenko, S.P., Gere, J.M. (1961). *Theory of Elastic Stability, 2nd Edition*, McGraw Hill, New York.

Williams, R.L., Lawrence, D.A. (2007). *Linear State-Space Control Systems*, John Wiley & Sons, New Jersey.

Wong, K.K.F., Hart, G.C. (1999a). "Inelastic earthquake control of weld failure I – Limit state approach." *The Structural Design of Tall Buildings*, 8 (4) 289-306.

Wong, K.K.F., Hart, G.C. (1999b). "Inelastic earthquake control of weld failure II – Probability theory." *The Structural Design of Tall Buildings*, 8 (4) 307-334.

Wong, K.K.F., Yang, R. (1999). "Inelastic dynamic response of structures using force analogy method." *Journal of Engineering Mechanics ASCE*, 125 (10) 1190-1199.

Wong, K.K.F., Wang Z. (2007a). "Seismic analysis of inelastic moment-resisting frames Part I: Modified force analogy method for end offsets." *The Structural Design of Tall and Special Buildings*, 16 (3) 267-282.

Wong, K.K.F., Wang Z. (2007b). "Seismic analysis of inelastic moment-resisting frames Part II: Energy dissipation in deformable panel zones." *The Structural Design of Tall and Special Buildings*, 16 (3) 283-299.

Wong, K.K.F. (2011). "Seismic energy analysis of structures with nonlinear fluid viscous dampers – Algorithm and numerical verification." *The Structural Design of Tall and Special Buildings*, 20 (4) 482-496.

Wong, K.K.F. (2014). "A new analytical method for solving nonlinear stability problems of framed structures." *Proceedings of the 2014 Annual Stability Conference, Structural Stability Research Council*, Toronto, Canada, Paper No. 5, 68-87.